Decentralized Optimal Projected Control of PV Inverters in Residential Microgrids ⋆

Pulkit Nahata [*,**] **Silvia Mastellone** [**] **Florian Dörfler** [*]

[*] *Automatic Control Lab, Swiss Federal Institute of Technology, 8092 Zurich, Switzerland (e-mail: {pnahata,dorfler}@ethz.ch).*
[**] *Control and Optimization Group, ABB Corporate Research, 5094 Baden, Switzerland (e-mail: silvia.mastellone@ch.abb.com)*

Abstract: In this paper, we consider the problem of overvoltage arising in PV residential microgrids due to excessive power injection into the grid by the PV generators. We propose a decentralized optimal integral controller to curtail excess active power in order to avoid overvoltage. Considering the voltage and active power constraints, we show that the proposed controller leads to maximum power injection into the grid. We discuss the objective of fair power curtailment and show that it is in contrast with our objective of maximum power transfer. Finally, we present the performance of the controller through simulation studies.

Keywords: decentralized control, renewable energy systems, solar energy, overvoltages.

1. INTRODUCTION

Since the past two decades, significant progress has been made in small-scale power generation and energy storage resulting in a reinvigorated interest in the idea of distributed generation. Apart from many advantages such as improved supply security, reduced power transmission losses, and increased standby capacity, the most important advantage lies in its compatibility with renewable sources of energy (Ackermann et al., 2001). With an increasing emphasis on sustainable energy, the recent series of legislations strongly favor the concept of distributed renewable based generation (Taylor et al., 2015).

Solar photovoltaic (PV) based generation is a commonly observed form of distributed generation in low voltage (LV) networks. However, a high PV penetration presents significant technical challenges in distribution networks. A typical household PV system generates more power than required by the load on a clear day and injects most of the generated power into grid. In some LV grids, the installed PV capacity can exceed the peak load by a factor of ten (Appen et al., 2013). The resulting reverse power flow causes a voltage rise in the distribution line. In case of intensive grid connection, this voltage rise may exceed the upper tolerance limit causing an overvoltage. In such a situation, the generating units need to be disconnected to avoid damage to the connected loads. An overvoltage is undesirable and needs to be addressed to ensure power quality.

To address these overvoltage issues, a few engineering approaches are used. A comprehensive overview of these approaches can be found in Tonkoski et al. (2010). One such approach is the curtailment of active power output of PV inverters in case of an overvoltage. We consider LV feeders where resistance/reactance (R/X) ratios are greater than one and can go up to twenty (Eur, 2015). Because of this resistive characteristic, the voltages are more sensitive to active power than reactive power (Yang et al., 2015). This makes the control of PV active power output a more suitable and effective method to mitigate the voltage-rise problem in LV networks.

The existing methods based on active power curtailment (APC) rely on either centralized or decentralized schemes. Centralized schemes (Pantziris, 2014) aim for control of the complete system from a centralized entity, for example, a distribution system control center. These schemes require global information which is often not possible in residential PV networks. Decentralized static droop control laws, based upon local measurements linearly trade off active power with respect to voltage, do not require communication between various PV generators (Tonkoski et al., 2011; Yang et al., 2015; Wang et al., 2012). The generators react to specific grid configuration according to predefined gains and local measurements at the inverter terminals. These are on-off control laws: they supply maximum power if the voltages are less than the critical voltage, and curtail power in case of an overvoltage. The power injection switches back to maximum as soon as the voltage goes below a certain critical voltage leading to chattering (voltage flicker).

The objective of the present work is to define a dynamic control solution that: 1) prevents overvoltage while avoiding chattering, 2) maximizes the power transfer, 3) has a decentralized control structure, and 4) guarantees stability of the closed loop system. The paper is organized as follows: Section 2 defines the network model and the overvoltage problem. The core result is presented in Section 3 where the decentralized optimal projected controller is presented. Section 4 presents a comparison of fair curtailment and maximum power injection objectives. Section 5 presents a case study and finally, Section 6 summarizes the conluding remarks and future work.

⋆ This research was supported by ABB Corporate Research, Switzerland and ETH Zürich.

Preliminaries and notation: Let $\mathbf{j} = \sqrt{-1}$ be the imaginary unit. Given $x \in \mathbb{R}^n$, let $[x] \in \mathbb{R}^{n\times n}$ be the associated diagonal matrix and $\bar{x}$ be its conjugate. $\mathbf{1}_n$ and $\mathbf{0}_n$ are n-dimensional vectors of all ones and zeros. $A \in \mathbb{R}^{n\times n}$ is a *Metzler* or M-matrix if $A_{ij} \leq 0 \; \forall \; i \neq j$ and all eigenvalues of A have positive real parts. In this case $A^{-1} \geq 0$, with strict inequality if A is *irreducible* (Berman and Plemmons, 1994). Given $u, v, w \in \mathbb{R}^n$ with $v_i \leq w_i, i = 1, \cdots, n$, we define the operator $[u]_v^w$ as the component-wise projection of u in the set $\{x \in \mathbb{R}^n : v_i \leq x_i \leq w_i, i = 1, \cdots, n\}$, i.e.,

$$[u]_v^w = \begin{cases} u_i & \text{if } v_i \leq u_i \leq w_i \\ v_i & \text{if } u_i < v_i \\ w_i & \text{if } u_i > w_i \end{cases} . \tag{1}$$

2. NETWORK MODELING AND PROBLEM SETUP

2.1 Network Modeling

Standard assumptions enabling positive sequence analysis are made. The residential grid consists of several houses connected to the utility grid via point of common coupling (PCC). We call these individual houses as nodes.

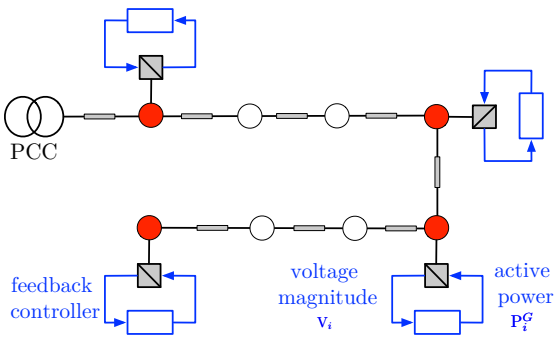

Fig. 1. A typical residential feeder. ● and ○ represent generating and load nodes respectively.

Fig. 1 shows a typical radial feeder in which a few houses are installed with PV generators while the others are pure loads. The sensing is available at the generating nodes and only these nodes are controlled. The grid is modeled as a linear circuit represented by a connected weighted graph $O(\mathcal{V}, \mathcal{E}, \mathcal{W})$ where $\mathcal{V} = \{0, \cdots, m+n\}$ is the set of vertices (nodes) and $\mathcal{E} \subseteq \mathcal{V} \times \mathcal{V}$ is the set of edges (branches). The node 0 denotes the PCC. The remaining nodes are classified as : $\mathcal{G} = \{1, \cdots, n\}, n \geq 1$ are the nodes with local generation to feed their loads, and $\mathcal{L} = \{n+1, \cdots, m+n\}, m \geq 1$ are the nodes which are pure loads, such that $\mathcal{V} = \mathcal{G} \cup \mathcal{L} \cup \{0\}$. Additionally, we define set $\mathcal{F} = \mathcal{G} \cup \mathcal{L}$.

Let $z_{ij} = r_{ij} + \mathbf{j}x_{ij} \in \mathbb{C}$ be the impedance between node i and j, where $r_{ij} \in \mathbb{R}_{>0}$ is the resistance and $x_{ij} \in \mathbb{R}_{>0}$ is the inductive reactance. The edge weights of the associated graph are the associated admittances $y_{ij} = g_{ij} + \mathbf{j}b_{ij} \in \mathbb{C}$, where $g_{ij} = r_{ij}/(r_{ij}^2 + x_{ij}^2) \in \mathbb{R}_{>0}$ is the associated conductance and $b_{ij} = -x_{ij}/(r_{ij}^2 + x_{ij}^2) \in \mathbb{R}_{<0}$ the susceptance. Owing to high resistances in LV networks, we neglect the shunt reactances in our model. The network is represented by symmetric admittance matrix $Y \in \mathbb{C}^{m+n+1\times m+n+1}$, where the off-diagonal elements are given by $Y_{ij} = Y_{ij} = -y_{ij}$ for each branch $\{i,j\} \in \mathcal{E}$ (0 if $\{i,j\} \notin \mathcal{E}$), and the diagonal elements are given by $Y_{ii} = \sum_{i=0, i\neq j}^{m+n} y_{ij}$. We represent $Y = G + \mathbf{j}B$, where G and B respectively are the conductance and susceptance matrices. It should be noted that $G_{ii} = \sum_{i=0, i\neq j}^{m+n} g_{ij} > 0$ and $G_{ij} = -g_{ij} < 0$.

To each node $i \in \mathcal{V}$, we associate a phasor voltage $E_i = V_i e^{\mathbf{j}\theta_i}$ and complex power $S_i = P_i + \mathbf{j}Q_i$. The active power P_i further depends upon the type of node:

$$P_i = \begin{cases} P_i^G + P_i^L & \text{if } i \in \mathcal{G} \\ P_i^L & \text{if } i \in \mathcal{L} \end{cases},$$

where $P_i^G \geq 0$ and $P_i^L \leq 0$ respectively are the active powers generated and consumed at a node. Since the conductors are made of the same material, the R/X exhibits a small variation and is assumed to be constant (Kersting, 2001). We define R/X to be constant, $1/\gamma$, where $0 < \gamma \ll 1$. This implies that $g_{ij}/b_{ij} = -1/\gamma$ and hence, $B = -\gamma G$. The power flow equations are obtained from Kirchhoffs and Ohms laws:

$$S = [E]G\bar{E} - \mathbf{j}[E]B\bar{E} = [E]G\bar{E} + \mathbf{j}\gamma[E]G\bar{E}. \tag{2}$$

These power flow equations are highly non-linear. Since the distribution networks are predominantly resistive in nature, the voltage profile is nearly flat. It is shown in (Bolognani and Dörfler, 2015) that by linearizing the power flow equations around a flat voltage profile (corresponding to a no-load condition of the grid), one obtains the relation:

$$\begin{bmatrix} G & \gamma G \\ \gamma G & -G \end{bmatrix} \begin{bmatrix} V \\ \theta \end{bmatrix} = \begin{bmatrix} P \\ Q \end{bmatrix}, \tag{3}$$

where V and θ are vectors of voltage magnitudes and phase angles. $G \in \mathbb{R}^{m+n+1\times m+n+1}$ is a Laplacian matrix and is positive semidefinite. The node 0 is modeled as a slack bus and its voltage and phase are assumed to be known and constant, $E_0 = V_0 e^{\mathbf{j}0}$. Since V_0 and θ_0 are already known, node 0 can be eliminated from (3). On partitioning (3) into sets $\{0\}$ and $\mathcal{F}$, it can be rewritten as:

$$\begin{bmatrix} G_{00} & G_{0\mathcal{F}} & \gamma G_{00} & \gamma G_{0\mathcal{F}} \\ G_{\mathcal{F}0} & G_{\mathcal{F}\mathcal{F}} & \gamma G_{\mathcal{F}0} & \gamma G_{\mathcal{F}\mathcal{F}} \\ \gamma G_{00} & \gamma G_{0\mathcal{F}} & -G_{00} & -G_{0\mathcal{F}} \\ \gamma G_{\mathcal{F}0} & \gamma G_{\mathcal{F}\mathcal{F}} & -G_{\mathcal{F}0} & -G_{\mathcal{F}\mathcal{F}} \end{bmatrix} \begin{bmatrix} V_0 \\ V_\mathcal{F} \\ \theta_0 \\ \theta_\mathcal{F} \end{bmatrix} = \begin{bmatrix} P_0 \\ P_\mathcal{F} \\ Q_0 \\ Q_\mathcal{F} \end{bmatrix}.$$

$G\mathbf{1}_{m+n+1} = \mathbf{0}_{m+n+1}$ and therefore, $G_{\mathcal{F}0} = -G_{\mathcal{F}\mathcal{F}}\mathbf{1}_{m+n}$. On substituting $\theta_0 = 0$, $P_\mathcal{F}$ and $Q_\mathcal{F}$ are obtained as:

$$-G_{\mathcal{F}\mathcal{F}}\mathbf{1}_{m+n}V_0 + G_{\mathcal{F}\mathcal{F}}V_\mathcal{F} + \gamma G_{\mathcal{F}\mathcal{F}}\theta_\mathcal{F} = P_\mathcal{F} \tag{4a}$$

$$-\gamma G_{\mathcal{F}\mathcal{F}}\mathbf{1}_{m+n}V_0 + \gamma G_{\mathcal{F}\mathcal{F}}V_\mathcal{F} - G_{\mathcal{F}\mathcal{F}}\theta_\mathcal{F} = Q_\mathcal{F}. \tag{4b}$$

The above equations represent the power flow without the PCC.

Lemma 1. The matrix $G_{\mathcal{F}\mathcal{F}}$ is an irreducible, positive definite, and M-matrix. Its inverse $G_{\mathcal{F}\mathcal{F}}^{-1}$ is well defined, positive, and positive definite.

Lemma 2. Let A be the inverse of an irreducible M-matrix such that

$$A = \begin{bmatrix} A_1 & A_2 \\ A_3 & A_4 \end{bmatrix}.$$

The following hold true:
(1) The Schur complements of A, $A/A_4 = A_1 - A_2A_4^{-1}A_3$ and $A/A_1 = A_4 - A_3A_1^{-1}A_2$ are positive.
(2) The matrices $A_3A_1^{-1}$ and $A_2A_4^{-1}$ are non-negative.

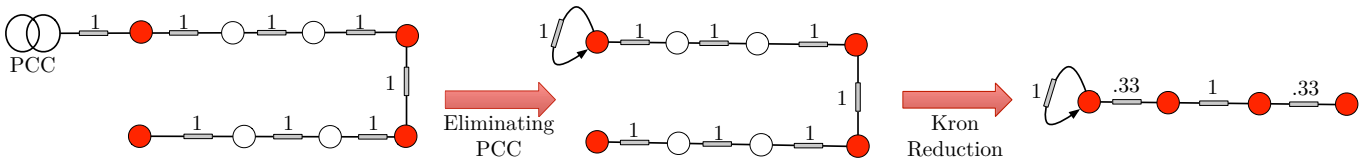

Fig. 2. A representative diagram of network reduction performed on feeder in Fig. 1 with unit conductances.

Proof. The proof of above Lemmas are omitted in this paper due to space constraints (Nahata, 2016). ■

The invertibility of $G_{\mathcal{F}\mathcal{F}}$ enables us to substitute $\theta_{\mathcal{F}} = G_{\mathcal{F}\mathcal{F}}^{-1}(-\gamma G_{\mathcal{F}\mathcal{F}}\mathbf{1}_{m+n}V_0 + \gamma G_{\mathcal{F}\mathcal{F}}V_{\mathcal{F}} - Q_{\mathcal{F}})$ in (4a). The explicit relationship between $V_{\mathcal{F}}$ and $P_{\mathcal{F}}$ can be written as:

$$G_{\mathcal{F}\mathcal{F}}V_{\mathcal{F}} = \beta P_{\mathcal{F}} + D, \tag{5}$$

where $\beta = \dfrac{1}{1+\gamma^2}, D = \gamma\beta Q_{\mathcal{F}} + G_{\mathcal{F}\mathcal{F}}\mathbf{1}_{m+n}V_0$. $Q_{\mathcal{F}} \in \mathbb{R}^{m+n\times 1}$ represents net reactive power at various nodes and is assumed to be constant. The PV inverters are assumed to operate close to unity power factor and predominantly generate active power.

2.2 Network Reduction

Each generating unit can sense nodal voltage and active power generated. We use network reduction to find an explicit relationship between the sensed parameters and to eliminate the rest. Since $\mathcal{F} = \mathcal{G} \cup \mathcal{L}$, on partitioning $G_{\mathcal{F}\mathcal{F}}$ into $\mathcal{G}$ and $\mathcal{L}$, (5) can be written as:

$$\begin{bmatrix} G_{\mathcal{G}\mathcal{G}} & G_{\mathcal{G}\mathcal{L}} \\ G_{\mathcal{L}\mathcal{G}} & G_{\mathcal{L}\mathcal{L}} \end{bmatrix} \begin{bmatrix} V_{\mathcal{G}} \\ V_{\mathcal{L}} \end{bmatrix} = \beta \begin{bmatrix} P_{\mathcal{G}}^G + P_{\mathcal{G}}^L \\ P_{\mathcal{L}}^L \end{bmatrix} + \begin{bmatrix} D_{\mathcal{G}} \\ D_{\mathcal{L}} \end{bmatrix}.$$

On the above matrix, we perform Kron reduction (Dörfler and Bullo, 2013) and eliminate $V_{\mathcal{L}}$. On substituting $V_{\mathcal{L}} = -G_{\mathcal{L}\mathcal{L}}^{-1}G_{\mathcal{L}\mathcal{G}}V_{\mathcal{G}} + \beta G_{\mathcal{L}\mathcal{L}}^{-1}P_{\mathcal{L}}^L + G_{\mathcal{L}\mathcal{L}}^{-1}D_{\mathcal{L}}$ in the upper block, we obtain:

$$V_{\mathcal{G}} = \beta\tilde{G}_{\mathcal{G}\mathcal{G}}^{-1}P_{\mathcal{G}}^G + D'_{\mathcal{G}}, \tag{6}$$

where $D'_{\mathcal{G}} = \beta P_{\mathcal{G}}^L + D_{\mathcal{G}} - \beta G_{\mathcal{G}\mathcal{L}}G_{\mathcal{L}\mathcal{L}}^{-1}P_{\mathcal{L}}^L - G_{\mathcal{G}\mathcal{L}}G_{\mathcal{L}\mathcal{L}}^{-1}D_{\mathcal{L}}$ and $\tilde{G}_{\mathcal{G}\mathcal{G}} = G_{\mathcal{G}\mathcal{G}} - G_{\mathcal{G}\mathcal{L}}G_{\mathcal{L}\mathcal{L}}^{-1}G_{\mathcal{L}\mathcal{G}}$. $\tilde{G}_{\mathcal{G}\mathcal{G}} = G_{\mathcal{F}\mathcal{F}}/G_{\mathcal{L}\mathcal{L}}$ is the Schur Complement of $G_{\mathcal{F}\mathcal{F}}$ with respect to $G_{\mathcal{L}\mathcal{L}}$. The matrix $\tilde{G}_{\mathcal{G}\mathcal{G}}$ is irreducible, positive definite, and M-matrix as these properties are closed under Schur complementation (Dörfler and Bullo, 2013). Its inverse $\tilde{G}_{\mathcal{G}\mathcal{G}}^{-1}$ is well defined, positive and positive definite. A representative diagram of network reduction is shown in Fig. 2.

2.3 The Overvoltage Problem

Definition 3. A node is said to be experiencing overvoltage if its voltage rises beyond a critical voltage V_i^* defined by grid standards.

Remark 4. In (6), the relation between voltage and power is defined by a positive matrix. An increase in active power of a generating node results in rise in voltages at all the nodes in the network.

Lemma 5. (**Overvoltage in radial feeders**). For all net generating nodes in a purely radial feeder, the farthest node from the PCC suffers from maximum overvoltage.

Proof. If all nodes are equipped with generation, $m = 0$. The nodes are numbered from $\{1 \cdots n\}$ such that 1 represents the node closest to PCC and n the farthest. For a radial feeder, the matrix $G_{\mathcal{F}\mathcal{F}}$ is a diagonally dominant tridiagonal M-matrix with zero row sums except for the first row. The inverse of such a matrix is not only positive but its elements decay along each row and column (Nabben, 1999, Corollary 3.4). Let g'_{ij} represent the elements of $G_{\mathcal{F}\mathcal{F}}^{-1}$. The elements of $G_{\mathcal{F}\mathcal{F}}^{-1}$ satisfy:

$$g'_{ii} < g'_{jj} \text{ if } i < j,\ g'_{ij} < g'_{ii} \text{ if } j > i,\ g'_{ij} = g'_{ii} \text{ if } i > j. \tag{7}$$

For low voltage networks $0 < \gamma \ll 1$, and $\gamma\beta Q_{\mathcal{F}}$ can be neglected. (5) can be written as:

$$V_{\mathcal{F}} = G_{\mathcal{F}\mathcal{F}}^{-1}P_{\mathcal{F}} + \mathbf{1}_n V_0. \tag{8}$$

On combining (7) and (8), the voltages satisfy:

$$V_i = V_{i-1} + \sum_{j=i}^{j=n} \vartheta_{ij}P_j,$$

where $\vartheta_{ij} = g'_{ij} - g'_{i-1,j} = \begin{cases} = 0 & \text{if } i > j, i > 1 \\ > 0 & \text{if } i \le j, i > 1 \end{cases}$. Hence, if all the nodes are net generating, $P_i > 0$. Thus, $V_n > V_{n-1} > \cdots > V_1$. ■

Definition 6. The *critical power* $P_{\mathcal{G}}^* \in \mathbb{R}^n$ is the power corresponding to the critical voltage vector V^*. Using (6), the relationship between $P_{\mathcal{G}}^*$ and the critical voltage V^* can be expressed as:

$$P_{\mathcal{G}}^* = (1/\beta)(\tilde{G}_{\mathcal{G}\mathcal{G}}V^* - D'_{\mathcal{G}}). \tag{9}$$

3. PROJECTED INTEGRAL CONTROLLER

The main aim of an APC based decentralized overvoltage control for PV generators is to inject power until the critical voltage is attained. Any further injection would increase the voltage beyond the critical value. However, tracking of critical voltage may not be feasible during periods of low generation. A projection operation takes into account the power constraints. We define a discrete-time projected integral controller as:

$$P_{\mathcal{G}}^G(t+1) = [P_{\mathcal{G}}^G(t) + \epsilon(V^* - V_{\mathcal{G}}(t))]_{\mathcal{P}}^+, \tag{10}$$

where ϵ is the droop coefficient, $V^* \in \mathbb{R}^{n\times 1}$ is the critical voltage, and the set $\mathcal{P} \subset \mathbb{R}^n$ is time-varying, convex, and defines the maximum power generation capacity of the PV generator.

Remark 7. (**The set $\mathcal{P}$ and projection operation**) The maximum power output of a PV generator is defined by $\bar{P}_i(t)$, and is varying in time due to changing irradiation. At a given time instant t, the inverter can inject any power between 0 and $\bar{P}_i(t)$. Thus, for a PV inverter, the power constraint set is $\mathcal{P} = \{P_{\mathcal{G}}^G : 0 \le (P_{\mathcal{G}}^G)_i \le \bar{P}_i, i \in \mathcal{G}\}$.

Since the set $\mathcal{P}$ is defined by linear inequalities, the projection operation, $[P_{\mathcal{G}}^G(t) + \epsilon(V^* - V_{\mathcal{G}}(t))]_{\mathcal{P}}^+$, is the

component-wise projection (as defined in (1)) of $P_{\mathcal{G}}^G(t) + \epsilon(V^* - V_{\mathcal{G}}(t))$ on set $\mathcal{P}$ and is defined as:

$$[P_{\mathcal{G}}^G(t) + \epsilon(V^* - V_{\mathcal{G}}(t))]_{\mathcal{P}}^{+} = [P_{\mathcal{G}}^G(t) + \epsilon(V^* - V_{\mathcal{G}}(t))]_0^{\bar{P}_{\mathcal{G}}}.$$

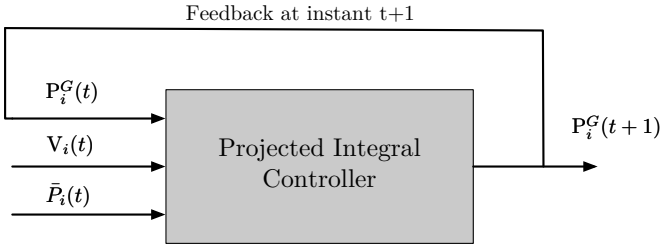

Fig. 3. Projected Integral Controller at i^{th} node.

Remark 8. At time t, each voltage controller needs only local measurements of voltage $V_i(t)$ and injected power $P_i^G(t)$ along with an estimate of its maximum power output $\bar{P}_i(t)$ required to perform the projection operation.

On combining (6), (9), and (10), we obtain the projected closed-loop dynamics (Hauswirth et al., 2016) as:

$$P_{\mathcal{G}}^G(t+1) = [P_{\mathcal{G}}^G(t) + \epsilon\beta\tilde{G}''_{\mathcal{G}\mathcal{G}}(P_{\mathcal{G}}^* - P_{\mathcal{G}}(t))]_{\mathcal{P}}^{+}, \tag{11}$$

where $\tilde{G}''_{\mathcal{G}\mathcal{G}} = \tilde{G}_{\mathcal{G}\mathcal{G}}^{-1}$ and $P_{\mathcal{G}}^*$ is defined in (9). The continuous-time version of (10) leads to hybrid closed-loop dynamics and is analyzed in Nahata et al. (2017).

Remark 9. (**Optimization problem for maximum power injection (MPI)**) If there were no power constraints, the critical power is the maximum power that can be injected to the grid. We consider the optimization problem which imposes quadratic penalty on the difference between critical power and generated power and is subject to the power constraints defined by set $\mathcal{P}$:

$$\begin{aligned} \min_x \quad & f(P_{\mathcal{G}}^G) = \frac{1}{2}(P_{\mathcal{G}}^* - P_{\mathcal{G}}^G)^T \tilde{G}''_{\mathcal{G}\mathcal{G}}(P_{\mathcal{G}}^* - P_{\mathcal{G}}^G) \\ \text{s.t.} \quad & P_{\mathcal{G}}^G \in \mathcal{P}, \end{aligned} \tag{12}$$

where $\mathcal{P} = \{P_{\mathcal{G}}^G : 0 \le (P_{\mathcal{G}}^G)_i \le \bar{P}_i, i \in \mathcal{G}\}$ is a convex set, $\tilde{G}''_{\mathcal{G}\mathcal{G}}$ is positive definite and (12) is strictly convex.

We will first consider the case of time-invariant $\mathcal{P}$ (constant maximum power output) and show how the closed-loop system converges to the optimal solution of (12), and later comment on the case of time varying $\mathcal{P}$.

Theorem 10. (**Decentralized projected integral controller under time-invariant $\mathcal{P}$**) Consider the closed-loop decentralized projected integral controller defined by the equation (11) and $\mathcal{P} = \{P_{\mathcal{G}}^G : 0 \le (P_{\mathcal{G}}^G)_i \le \bar{P}_i, i \in \mathcal{G}\}$. For $0 < \epsilon < 2/\beta\bar{\sigma}(\tilde{G}''_{\mathcal{G}\mathcal{G}})$, where $\bar{\sigma}(\tilde{G}''_{\mathcal{G}\mathcal{G}})$ is the maximum singular value of $\tilde{G}''_{\mathcal{G}\mathcal{G}}$, the following statements hold true:
1. The sequence $\{P_{\mathcal{G}}^G(t+1)\}$ generated by the controller converges to the optimum point of (12).
2. In equilibrium, all generator voltages are always less than or equal to the critical voltage.

Proof. To prove statement 1, we first write (11) as a projected gradient flow:

$$P_{\mathcal{G}}^G(t+1) = [P_{\mathcal{G}}^G(t) - \epsilon\beta\nabla f(P_{\mathcal{G}}^G)]_{\mathcal{P}}^{+},$$

where $\nabla f(P_{\mathcal{G}}^G) = -\tilde{G}''_{\mathcal{G}\mathcal{G}}(P_{\mathcal{G}}^* - P_{\mathcal{G}}^G)$ is the gradient of the function $f(P_{\mathcal{G}}^G)$ in (12). Since $P_{\mathcal{G}}^G(t+1)$ is the projection of $P_{\mathcal{G}}^G(t) - \epsilon\nabla f(P_{\mathcal{G}}^G)$ on set $\mathcal{P}$, using the projection theorem (Bertsekas, 1999), we obtain $(P_{\mathcal{G}}^G(t) - \epsilon\beta\nabla f(P_{\mathcal{G}}^G) - P_{\mathcal{G}}^G(t+1))^T(P_{\mathcal{G}}^G(t) - P_{\mathcal{G}}^G(t+1)) \le 0$. On simplifying further,

$$\begin{aligned} &(\nabla f(P_{\mathcal{G}}^G))^T(P_{\mathcal{G}}^G(t+1) - P_{\mathcal{G}}^G(t)) \\ &\qquad \le -\frac{1}{\epsilon\beta}\left\|P_{\mathcal{G}}^G(t+1) - P_{\mathcal{G}}^G(t)\right\|^2. \end{aligned} \tag{13}$$

Also, for all $P_{\mathcal{G}}^G$ and $\tilde{P}_{\mathcal{G}}^G \in \mathbb{R}^n$, $\left\|\nabla f(P_{\mathcal{G}}^G) - \nabla f(\tilde{P}_{\mathcal{G}}^G)\right\| \le \bar{\sigma}(\tilde{G}''_{\mathcal{G}\mathcal{G}})\left\|P_{\mathcal{G}}^G - \tilde{P}_{\mathcal{G}}^G\right\|$. The function $\nabla f(P_{\mathcal{G}}^G)$ is globally Lipschitz continuous in $P_{\mathcal{G}}^G$ which enables us to use the gradient descent Lemma (Bertsekas, 1999, Proposition A.24): $f(P_{\mathcal{G}}^G(t+1)) - f(P_{\mathcal{G}}^G(t)) \le (\nabla f(P_{\mathcal{G}}^G))^T(P_{\mathcal{G}}^G(t+1) - P_{\mathcal{G}}^G(t)) + \frac{\bar{\sigma}(\tilde{G}''_{\mathcal{G}\mathcal{G}})}{2}\left\|P_{\mathcal{G}}^G(t+1) - P_{\mathcal{G}}^G(t)\right\|^2$. On substituting (13), we obtain $f(P_{\mathcal{G}}^G(t+1)) - f(P_{\mathcal{G}}^G(t)) \le \left(-\frac{1}{\epsilon\beta} + \frac{\bar{\sigma}(\tilde{G}''_{\mathcal{G}\mathcal{G}})}{2}\right)\left\|P_{\mathcal{G}}^G(t+1) - P_{\mathcal{G}}^G(t)\right\|^2$. We can state that as long as $0 < \epsilon < 2/\beta\bar{\sigma}(\tilde{G}''_{\mathcal{G}\mathcal{G}})$, $f(P_{\mathcal{G}}^G(t+1)) - f(P_{\mathcal{G}}^G(t)) \le 0$, and the equality holds if and only if $P_{\mathcal{G}}^G(t+1) = P_{\mathcal{G}}^G(t)$. If the algorithm converges to $\hat{P}_{\mathcal{G}}^G \in \mathcal{P}$, then

$$[\hat{P}_{\mathcal{G}}^G - \epsilon\beta\nabla f(\hat{P}_{\mathcal{G}}^G)]_{\mathcal{P}}^{+} = \hat{P}_{\mathcal{G}}^G. \tag{14}$$

From the projection theorem (Bertsekas, 1999), equivalently:

$$(\hat{P}_{\mathcal{G}}^G - \epsilon\beta\nabla f(\hat{P}_{\mathcal{G}}^G) - \hat{P}_{\mathcal{G}}^G)^T(P_{\mathcal{G}}^G - \hat{P}_{\mathcal{G}}^G) \le 0 \quad \forall P_{\mathcal{G}}^G \in \mathcal{P}$$

$$(\nabla f(\hat{P}_{\mathcal{G}}^G))^T(P_{\mathcal{G}}^G - \hat{P}_{\mathcal{G}}^G) \ge 0 \quad \forall P_{\mathcal{G}}^G \in \mathcal{P}.$$

The above equation is the first order optimality condition. Since $f(P_{\mathcal{G}}^G)$ is the strictly convex, i is necessary and sufficient for $\hat{P}_{\mathcal{G}}^G$ to minimize $f(P_{\mathcal{G}}^G)$ over $\mathcal{P}$. This concludes the proof of the first statement.

Statement (2) can proved directly by further simplifying the steady state condition. We rewrite equation (3) as:

$$[\hat{P}_{\mathcal{G}}^G - \epsilon\beta\nabla f(\hat{P}_{\mathcal{G}}^G)]_{\mathcal{P}}^{+} = [\hat{P}_{\mathcal{G}}^G + \epsilon(V^* - \hat{V}_{\mathcal{G}})]_0^{\bar{P}_{\mathcal{G}}} = \hat{P}_{\mathcal{G}}^G.$$

On writing the above equation element-wise, we obtain:

$$[\hat{P}_i^G + \epsilon(V_i^* - \hat{V}_i)]_0^{\bar{P}_i} = \hat{P}_i^G \quad i \in \mathcal{G}. \tag{15}$$

The above equation defines the condition that must hold true when (11) converges. We now consider the possible cases of nodal voltages and the corresponding powers:

(1) If $\hat{V}_i = V_i^*$, then $[\hat{P}_i^G]_0^{\bar{P}} = \hat{P}_i^G$. This can only hold true if $0 \le \hat{P}_i \le \bar{P}_i$. The node i is unsaturated.
(2) If $\hat{V}_i < V_i^*$, then $\epsilon(V_i^* - \hat{V}_i) > 0$. (15) holds true if and only if $\hat{P}_i = \bar{P}_i$. Thus, the nodes i is saturated.
(3) If $\hat{V}_i > V_i^*$, then $\epsilon(V_i^* - \hat{V}_i) < 0$. (15) holds true if and only if $\hat{P}_i = 0$.

We will now consider the third case of $\hat{P}_i = 0$. Let the set $\mathcal{X}$ and $\mathcal{Y}$ represent the sets with zero and non-zero power generation respectively. It can be shown that $V_{\mathcal{X}} = V_{\mathcal{X}}^* - \beta(\tilde{G}''_{\mathcal{X}\mathcal{X}} - \tilde{G}''_{\mathcal{X}\mathcal{Y}}\tilde{G}''^{-1}_{\mathcal{Y}\mathcal{Y}}\tilde{G}''_{\mathcal{Y}\mathcal{X}})P_{\mathcal{X}}^* - \tilde{G}''_{\mathcal{X}\mathcal{Y}}\tilde{G}''^{-1}_{\mathcal{Y}\mathcal{Y}}(V_{\mathcal{Y}}^* - V_{\mathcal{Y}})$. From Lemma 2, $(\tilde{G}''_{\mathcal{X}\mathcal{X}} - \tilde{G}''_{\mathcal{X}\mathcal{Y}}\tilde{G}''^{-1}_{\mathcal{Y}\mathcal{Y}}\tilde{G}''_{\mathcal{Y}\mathcal{X}})$ and $\tilde{G}''_{\mathcal{X}\mathcal{Y}}\tilde{G}''^{-1}_{\mathcal{Y}\mathcal{Y}}$ are respectively positive and non-negative. As $P_{\mathcal{X}}^* \ge 0$ and $V_{\mathcal{Y}} \le V_{\mathcal{Y}}^*$, it follows that $V_{\mathcal{X}} \le V_{\mathcal{X}}^*$. It can be stated that (11) always converges to voltages less than or equal to the critical voltage for all the nodes. ■

Remark 11. (**Case of time varying** $\mathcal{P}$) The controller (11) converges to $\hat{P}_{\mathcal{G}}^G$ such that it is the projection of $\hat{P}_{\mathcal{G}}^G - \epsilon\nabla f(\hat{P}_{\mathcal{G}}^G)$ on $\mathcal{P}$. When $\mathcal{P}$ changes overtime to $\bar{\mathcal{P}}$, $\hat{P}_{\mathcal{G}}^G$ remains the optimal point if and only if

$$\hat{P}_{\mathcal{G}}^G = [\hat{P}_{\mathcal{G}}^G - \epsilon\nabla f(\hat{P}_{\mathcal{G}}^G)]_{\mathcal{P}}^+ = [\hat{P}_{\mathcal{G}}^G - \epsilon\nabla f(\hat{P}_{\mathcal{G}}^G)]_{\bar{\mathcal{P}}}^+.$$

This can happen in a few cases, for example, if the new power constraint set $\bar{\mathcal{P}}$ is defined by an increase in $\bar{P}_i(t)$ of only the unsaturated nodes. In such a scenario, the projection of $\hat{P}_{\mathcal{G}}^G - \epsilon\nabla f(\hat{P}_{\mathcal{G}}^G)$ on $\bar{\mathcal{P}}$ will be same as on $\mathcal{P}$, and the optimal injections with respect to $\mathcal{P}$ are also optimal with respect to $\bar{\mathcal{P}}$. Otherwise, the controller will increase or decrease power injections at different nodes and converges to a new optimum.

4. FAIR CURTAILMENT OF ACTIVE POWER

The proposed controller (10) curtails power with respect to the difference of nodal voltage with critical voltage. The nodes farther away from PCC experience a higher voltage rise as compared to nodes which are closer, and therefore suffer from more curtailment (see Section 5 for a case study). such a curtailment unfair in the sense that despite available generation capacity, a generating node has to curtail more than the others based upon its location within the residential network. To address this issue, the concept of fair curtailment is introduced which aims at curtailment in proportion to maximum power generation capacity $\bar{P}_i$ of the node (Ali et al., 2015).

Definition 12. The curtailment is said to be fair if in case the voltage of any of the generating nodes in the network exceeds the critical voltage, all the nodes curtail power proportional to its capacity,

$$\frac{\bar{P}_i - P_i^G}{\bar{P}_i} = \frac{\bar{P}_j - P_j^G}{\bar{P}_j} \qquad \forall i, j \in \mathcal{G}, \tag{16}$$

to achieve $V_{\mathcal{G}} \leq V^*$.

Lemma 13. Power injections based on fair curtailment are not optimal with respect to the goal of MPI defined by (12).

Proof. We know that closed-loop system defined in (11) converges to the optimum point of (12). Assume the equilibria of closed-loop system under fair curtailment and MPI coincide with each other. This is only true when both (15) and (16) simultaneously hold true. In case of an overvoltage, let the equilibrium curtailment be $\Delta P_i^G = \bar{P}_i - P_i^G > 0$ per node. Consider a partition of the nodes $\mathcal{S} \cup \mathcal{N} = \mathcal{G}$ of $\mathcal{G}$ such that $V_{\mathcal{S}} < V_{\mathcal{S}}^*$ and $V_{\mathcal{N}} = V_{\mathcal{N}}^*$. Under our assumption, the equilibria of both the controllers coincide and also holds true for $i \in \mathcal{S}$. Therefore,

$$[\bar{P}_i - \Delta P_i^G + \epsilon(V_i^* - V_i)]_0^{\bar{P}_i} = \bar{P}_i - \Delta P_i^G \quad i \in \mathcal{S}.$$

Recall from (1) that the left hand side can be: $\bar{P}_i - \Delta P_i^G + \epsilon(V_i^* - V_i)$, $\bar{P}_i$, or 0. The above equation has a solution if and only if $\Delta P_i^G = 0$ and has no solution for non-zero curtailment for all nodes. This is a contradiction to our assumption as the equilibrium condition does not hold for all $i \in \mathcal{G}$. As equations (15) and (16) do not simultaneously hold true, the fair curtailment based controller does not converge to the optimum point of (12). ■

The fair curtailment problems have been approached in literature through sensitivity based analysis which requires prior knowledge about the grid topology and parameters (Ali et al., 2015; Tonkoski et al., 2010). In case of networks with decentralized generators of different capacities, the instantaneous maximum power generation needs to be updated requiring communication. Fair curtailment puts an additional burden of communication on the generating nodes, requires an accurate knowledge of grid parameters, grid topology, and pre-computed load flow solutions. It also does not maximize power injected into the grid.

5. CASE STUDY

In this Section, we show the performance of the proposed controller using the nonlinear AC power flow equations defined in (2) and its effectiveness in mitigating overvoltage problem in LV networks. The system comprises of a radial distribution feeder and three houses (see Fig. 4) inspired from the Canadian residential feeder presented in Tonkoski et al. (2011). The critical voltage is chosen as 1.06 p.u. with 1 p.u. as the base voltage.

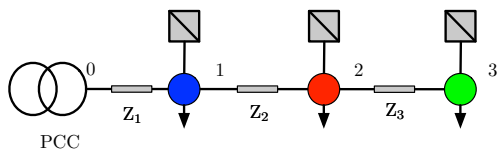

Fig. 4. A radial distribution feeder with three houses.

Fig. 5 shows the approximate load and PV profiles which are assumed to be identical for all the houses. Fig. 6 shows

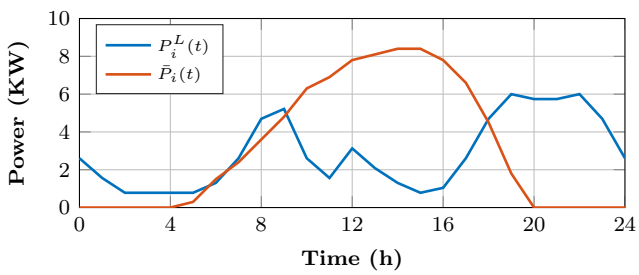

Fig. 5. PV generation and approximate load at each house.

comparison between MPI and fair curtailment objectives. Both the control schemes are able to mitigate overvoltage (Fig. 6a). The MPI objective can be attained in a decentralized fashion where as fair curtailment requires input from sensitivity analysis and pre-computed load flow solutions presented in Ali et al. (2015); Tonkoski et al. (2010). Since $\bar{P}_i$ of all PV generators is same, they experience the same curtailment under the fair curtailment objective as shown in Fig. 6b. The MPI objective results in more curtailment for farther away nodes (see also Lemma 5). It should be noted that fair curtailment results in active power curtailment as soon as the third node experiences overvoltage where as this is not true in case of MPI objective. Fig. 6c shows that fair curtailment results in less power export to the utility grid as compared to the MPI objective attained by discrete-time projected integral controller.

Fair curtailment results in further reduction in power injection for long line lengths which is typically the case in rural LV networks. This is because the voltage of a node

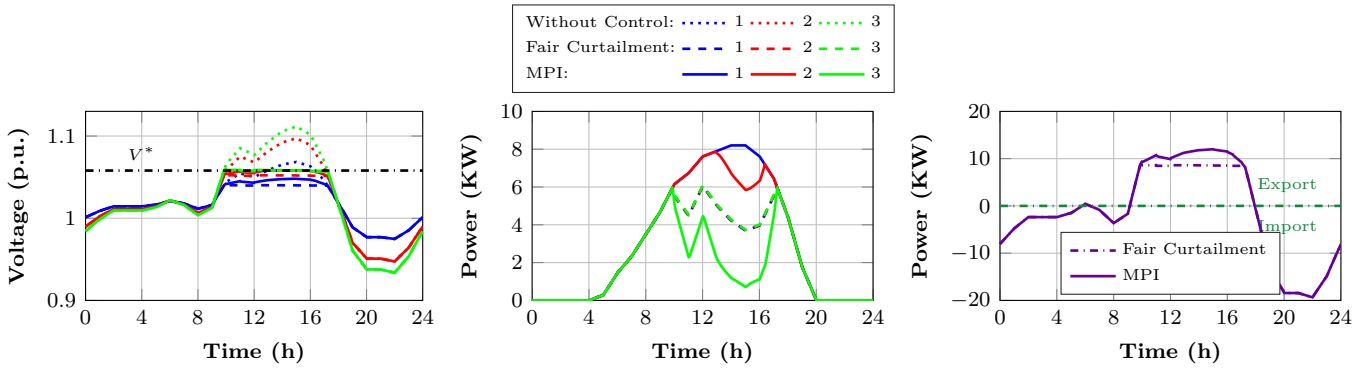

(a) Voltage profiles of various generating nodes.

(b) Active power output of PV Generators.

(c) Power flowing through PCC.

Fig. 6. Voltage profiles, nodal generation, and power transfer through PCC.

is more sensitive to its power generation/consumption than the other nodes in the network (see (7)). Since the curtailment is distributed over all the nodes in the fair curtailment objective, it generally leads to more power curtailment (see Nahata (2016) for a case study).

6. CONCLUSION

We studied the problem of overvoltage prevention in PV residential microgrids. A decentralized optimal integral projected controller was proposed to prevent overvoltage while maximizing the power transfer. Each PV generator controls the voltage using only local voltage and power measurements. This control strategy is especially valuable as it does not require a central coordinator nor communication between the generators. We also showed how the problem of maximum power injection conflicts with the fair curtailment of power by the generators, hence demonstrating that the fair curtailment problem requires different means to be addressed such as economical redistribution or use of local energy storage during periods of overvoltage.

REFERENCES

(2015). European Low Voltage Test Feeders. `https://ewh.ieee.org/soc/pes/dsacom/testfeeders`.

Ackermann, T., Andersson, G., and Sder, L. (2001). Distributed generation: a definition. *Electric Power Systems Research*, 57(3), 195 – 204.

Ali, M.M.V.M., Nguyen, P.H., Kling, W.L., Chrysochos, A.I., Papadopoulos, T.A., and Papagiannis, G.K. (2015). Fair power curtailment of distributed renewable energy sources to mitigate overvoltages in low-voltage networks. In *PowerTech, 2015 IEEE Eindhoven*, 1–5.

Appen, J.V., Braun, M., Stetz, T., Diwold, K., and Geibel, D. (2013). Time in the sun: the challenge of high PV penetration in the german electric grid. *IEEE Power and Energy Magazine*, 11(2), 55–64.

Berman, A. and Plemmons, R. (1994). *Nonnegative Matrices in the Mathematical Sciences*. Society for Industrial and Applied Mathematics.

Bertsekas, D.P. (1999). *Nonlinear Programming*. Athena Scientific.

Bolognani, S. and Dörfler, F. (2015). Fast power system analysis via implicit linearization of the power flow manifold. In *Allerton Conference on Communication, Control, and Computing*, 8.

Dörfler, F. and Bullo, F. (2013). Kron reduction of graphs with application to electrical networks. *IEEE Transactions on Circuits ad Systems 1: Regular papers*, 60(1), 150 – 163.

Hauswirth, A., Bolognani, S., Hug, G., and Dörfler, F. (2016). Projected gradient descent on riemannian manifolds with applications to online power system optimization. In *Allerton Conf. on Communications, Control and Computing*.

Kersting, W.H. (2001). Radial distribution test feeders. *IEEE Power Engineering Society Winter Meeting*, 2, 908–912.

Nabben, R. (1999). Decay rates of the inverse of nonsymmetric tridiagonal and band matrices. *SIAM Journal on Matrix Analysis and Applications*, 20(3), 820–837.

Nahata, P. (2016). *Decentralized Active Power Control of PV Inverters in Residential Microgrids*. Master's thesis, ETH Zürich.

Nahata, P., Mastellone, S., and Dörfler, F. (2017). A decentralized switched system approach to overvoltage prevention in PV residential microgrids. In *IFAC World Congress*. To appear.

Pantziris, K. (2014). *Voltage support strategies in a rural low voltage network with high photovoltaic penetration*. Master's thesis, TU Delft.

Taylor, J.A., Dhople, S.V., and Callaway, D.S. (2015). Power systems without fuel. *CoRR*, abs/1506.04799.

Tonkoski, R., Lopes, L.A.C., and EL-Fouly, T.H.M. (2010). Droop-based active power curtailment for overvoltage prevention in grid connected pv inverters. In *2010 IEEE International Symposium on Industrial Electronics*, 2388–2393.

Tonkoski, R., Lopes, L.A.C., and El-Fouly, T.H.M. (2011). Coordinated active power curtailment of grid connected pv inverters for overvoltage prevention. *IEEE Transactions on Sustainable Energy*, 2(2), 139–147.

Wang, Y., Zhang, P., Li, W., Xiao, W., and Abdollahi, A. (2012). Online overvoltage prevention control of photovoltaic generators in microgrids. *IEEE Transactions on Smart Grid*, 3(4), 2071–2078.

Yang, G., Marra, F., Juamperez, M., Kjær, S., Hashemi, D., Østergaard, J., Ipsen, H., and Frederiksen, H. (2015). Voltage rise mitigation for solar PV integration at LV grids. *Journal of Modern Power Systems and Clean Energy*, 3(3), 411–421.